Journal of Hydrology 526 (2015) 68–77

Contents lists available at ScienceDirect

Journal of Hydrology

journal homepage: www.elsevier.com/locate/jhydrol

Exploration of drought evolution using numerical simulations over the Xijiang (West River) basin in South China

Jun Niu [a,b], Ji Chen [b,*], Liqun Sun [b]

[a] Centre for Agricultural Water Research in China, China Agricultural University, Beijing 100083, China
[b] Department of Civil Engineering, The University of Hong Kong, Pokfulam, Hong Kong, China

ARTICLE INFO

Article history:
Available online 18 November 2014

Keywords:
Drought evolution
Variable Infiltration Capacity (VIC) model
Standardized precipitation index (SPI)
Standardized runoff index (SRI)
Soil moisture anomaly index (SMAI)
South China

SUMMARY

The knowledge of drought evolution characteristics may aid the decision making process in mitigating drought impacts. This study uses a macro-scale hydrological model, Variable Infiltration Capacity (VIC) model, to simulate terrestrial hydrological processes over the Xijiang (West River) basin in South China. Three drought indices, namely standardized precipitation index (SPI), standardized runoff index (SRI), and soil moisture anomaly index (SMAI), are employed to examine the spatio-temporal and evolution features of drought events. SPI, SRI and SMAI represent meteorological drought, hydrological drought and agricultural drought, respectively. The results reveal that the drought severity depicted by SPI and SRI is similar with increasing timescales; SRI is close to that of SPI in the wet season for the Liu River basin as the high-frequency precipitation is conserved more by runoff; the time lags appear between SPI and SRI due to the delay response of runoff to precipitation variability for the You River basin. The case study in 2010 spring drought further shows that the spatio-temporal evolutions are modulated by the basin-scale topography. There is more consistency between meteorological and hydrological droughts for the fan-like basin with a converged river network. For the west area of the Xijiang basin with the high elevation, the hydrological drought severity is less than meteorological drought during the developing stage. The recovery of hydrological and agricultural droughts is slower than that of meteorological drought for basins with a longer mainstream.

1. Introduction

Drought is more nebulous than other water-related natural disasters, and it is difficult to describe its status and evolution, due to its inherent characteristics, such as slow onset and the complexity of its impacts (Svoboda et al., 2002). Three physical drought types (namely, meteorological drought, hydrological drought and agricultural drought) are associated with a water deficiency in the hydrological cycle (Keyantash and Dracup, 2002; Mishra and Singh, 2010; Dai, 2011). A below-normal precipitation relates to meteorological drought. Hydrological drought may occur when streamflow, reservoir storage, or groundwater heights fall below long-term mean levels. Agricultural drought mainly results from a deficiency of available water (e.g., soil moisture) for plant growth.

The endeavors to the drought depiction (e.g., Palmer, 1965; McKee et al, 1993), assessment (e.g., Soulé, 1992; Sheffield et al., 2004), monitoring (e.g., Kunkel, 1990; özger et al., 2009), and forecasting (e.g., Mishra et al., 2007; Mishra and Singh, 2009) are everlasting worldwide for the costliest natural disaster (Federal Emergency Management Agency (FEMA), 1995; Wilhite, 2000). The precise quantification of drought is an extremely challenging task, and there is no a general way to quantify drought severity due to the three physical forms of drought (Heim, 2002). Keyantash and Dracup (2002) listed the evaluation criteria (relative importance) in judging the overall utility of the drought indices: robustness (28%), tractability (21%), transparency (17%), sophistication (17%), extendability (10%), and dimensionality (7%). With the application of the weighted criteria, a range of drought indices were compared and discussed. The selected meteorological drought indices include cumulative precipitation anomalies, rainfall deciles, Palmer drought severity index (PDSI) (Palmer, 1965), drought area index (DAI) (Bhalme and Mooley, 1980), rainfall anomaly index (RAI) (van Rooy, 1965), and standardized precipitation index (SPI) (McKee et al, 1993). Total water deficit (Long et al, 2013), cumulative streamflow anomaly, Palmer hydrological drought severity index (PHDI), and surface water supply index (SWSI) (Shafer and Dezman, 1982) were used for the quantification of hydrological drought. Crop moisture index (CMI) (Palmer, 1968), Palmer moisture anomaly index (Z index),

* Corresponding author. Tel.: +852 2859 2646.
E-mail address: jichen@hku.hk (J. Chen).

http://dx.doi.org/10.1016/j.jhydrol.2014.11.029
0022-1694/

computed soil moisture, and soil moisture anomaly index (SMAI) (Bergman et al., 1988) were the representatives of agricultural drought indices. The comparison results show that the overall superior drought indices, of the subset of drought indices discussed, are rainfall deciles, total water deficit, and computed soil moisture for the meteorological, hydrological, and agricultural drought types respectively, followed by SPI, cumulative streamflow anomaly, and SMAI (ranked at the second place respectively).

Numerical modeling is an important tool to provide fundamental hydrological information for water-related researches by performing water balance assessment of the soil column, using the variables such as precipitation, air temperature, wind speed, soil porosity, and infiltration, for water-related studies (Huang et al., 1996; Chen and Kumar, 2001; Maurer et al., 2002; Chen and Wu, 2012). The basis of hydrological study is being advanced by the various kinds of modern techniques, such as the Digital Elevation Models (DEM) and the remote sensing of soil and vegetation information. The macro-scale hydrological models that incorporate sufficient physical processes to maintain both water and energy balances of the major components in the land surface have been applied over the catchment to continental levels. The utilization of land surface modeling scheme is highly suited to the analysis of the occurrence and intensity of drought, especially for a large-scale river basin (Sheffield et al., 2004; Wu et al., 2011). With the simulated runoff and soil moisture schemes, we can perform the relevant analysis on different time and spatial scales. Among the land surface models, the semi-distributed, physical based Variable Infiltration Capacity (VIC) model (Liang et al., 1994) has been applied to provide a long-term hydrologically based dataset of land surface fluxes and states for the conterminous United States (Maurer et al., 2002), and for analyzing historical drought events for the United States (Sheffield et al., 2004; Andreadis and Lettenmaier, 2006) and globally (e.g., Nijssen et al., 1997; Sheffield and Eric, 2008).

The Xijiang (West River) basin in South China (see Fig. 1) involves 8 sub-basins, namely the Guihe River, the Liu River, the Hongshui River, the Beipan River, the Nanpan River, the You River, and the Xijiang Lower Reach. The total drainage area of the basin is 353,000 km^2, which is about the 77.83% of the whole basin area, as the largest tributary of the Pearl River (Pearl River Water Resources Commission, 2005). The basin belongs to a sub-tropical to tropical monsoon climate region, and the mean annual precipitation and runoff are 1447 and 668.6 mm for the period of 1952–2000 (Niu and Chen, 2010), respectively, with the runoff ratio 0.46. The mean annual temperature ranged from 14 to 22 °C (for the west part and lower reach) (Niu et al., 2013). Although there is abundant precipitation over the basin, the spatio-temporal hydrological variabilities are substantial (Zhang et al., 2009; Chen et al., 2013; Niu, 2013). For example, 80% of the annual precipitation occurs in the wet season of April to September and only about 8% in winter (i.e., December, January, and February); the difference of annual precipitation between the Nanpan and Guihe River basins is about 217.9 mm. Because of the high variations, the drought events frequently occurred (Cui et al., 2007; Xiao et al., 2012). The disaster area for the Xijiang basin in the drought year 1963 is 1.62×10^6 - hectares, which is about 5% of the total basin area (Pearl River Hydraulic Research Institute, 2007). The trend and abrupt shift in the annual mean discharge of nine stations were analyzed in Zhang et al. (2008), and no significant trend was found at the annual timescale. Fischer et al. (2013) studied the long-time wet and dry variations in the Xijiang River basin. Among them, the standardized discharge index (SDI) was applied to study the drought features in the basin, but only performed on one discharge control station (Gaoyao) at 24-month timescale. The drought episodes and risks were studied, using SPI and return periods methods, for the Pearl River basin based on the daily precipitation data for the period of 1960–2005 by Zhang et al. (2013). The terrestrial hydrological processes over the whole Pearl River basin, for the period of 1952–2000, were simulated by Niu and Chen (2010). Niu et al. (2013) further extended the simulation for the period of 2001–2010 for the major tributary of the Pearl River, the Xijiang basin. The hydrological response to precipitation variability was revealed (Niu and Chen, 2014), with focusing on 1963 drought event, over two sub-basins: the Guihe River and the Nanpan River basins. The results show that the Nanpan River basin is more vulnerable to the meteorological drought.

Following up on the studies by Niu and Chen (2010, 2014) and Niu et al. (2013), the present study evaluates the drought severity over the Xijiang River in the forms of meteorological, hydrological, and agricultural droughts, by using the VIC model simulations, in order to improve our understanding of the regional evolution processes of drought events. Two specific questions we addressed are:

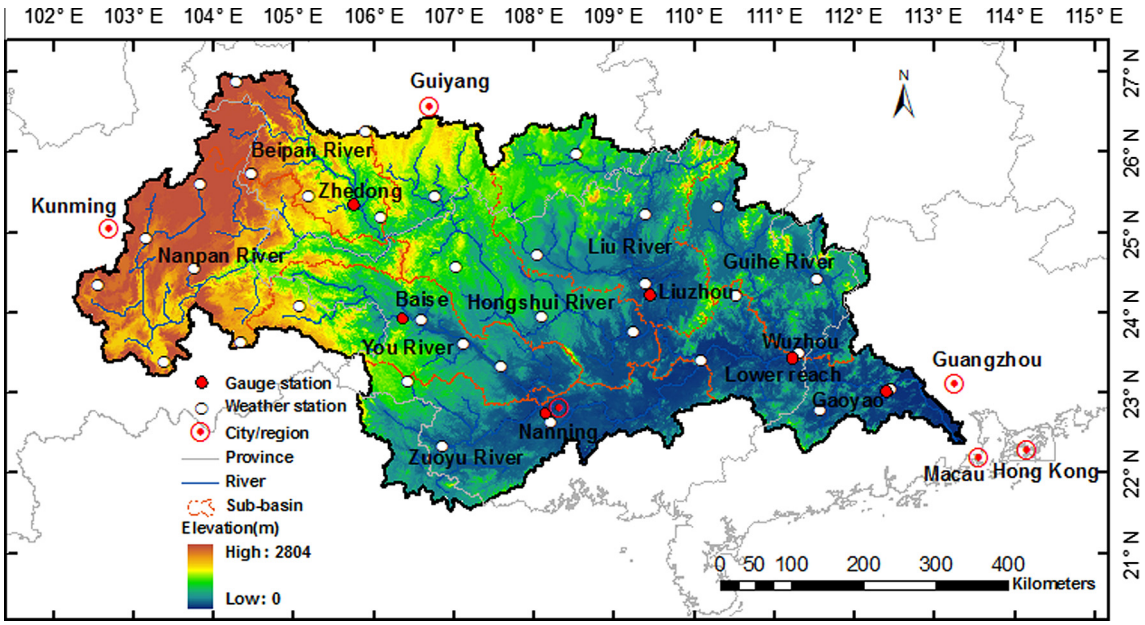

Fig. 1. The Xijiang basin in South China, weather/gauge stations, and its sub-basins.

(1) for the regional drought event in the Xijiang River, South China, what are the drought statuses of different drought forms? and (2) the possible influences of local topographic features to the drought evolution among the physical forms. To this end, the observed precipitation, simulated runoff and soil moisture are utilized to produce the severity indices for three different drought types accordingly. The SPI is used for meteorological drought, and the standardized runoff index (SRI) and soil moisture anomaly index (SMAI) are employed, for hydrological and agricultural drought, respectively, based on the VIC model simulations. The influences of basin-featured topography are mainly discussed on the five headwater sub-basins (i.e., the Guihe River, the Liu River, the Baipan River, the Nanpan River and the You River) in the Xijiang basin.

The rest of this paper is organized as follows. Section 2 describes the observed precipitation, and the runoff/soil moisture data simulated from the VIC model for this study. The description of different drought indices, including the SPI, SRI, and SMAI, is provided in Section 3. Section 4 presents the corresponding results of SPI and SRI indices over the period of 1952–2010 and a case study for a drought in March 2010 using SPI, SRI, and SMAI collectively. Conclusions are drawn in Section 5.

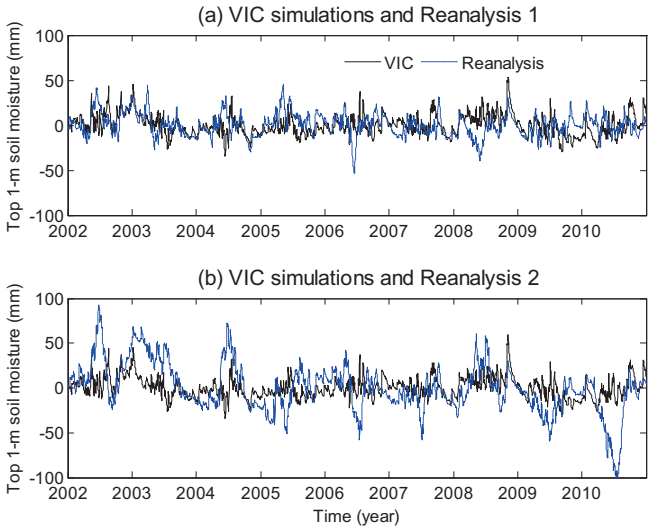

Fig. 2. (a) Comparisons of total top 1.5 m soil moisture between the VIC model simulations and NCEP-NCAR re-analysis-1 data (R-1) over the period of 2002–2010 for the Xijiang basin. (b) Same as (a) but with NCEP-DOE re-analysis-2 data (R-2).

2. Data

The terrestrial hydrological data (runoff and soil moisture) for studying the drought properties in the present study are from the VIC model (Liang et al., 1994) simulations. The modeling of terrestrial hydrological processes over the Xijiang basin for the periods of 1951–2000 and 2001–2010 has been reported in Niu and Chen (2010) and Niu et al. (2013) respectively. The period is separated due to the availability of forcing data. For the period of 1951–2000, the forcing meteorological data for the VIC model, including precipitation, maximum/minimum temperature, and wind speed, were obtained from Feng et al. (2004) at daily timescale with

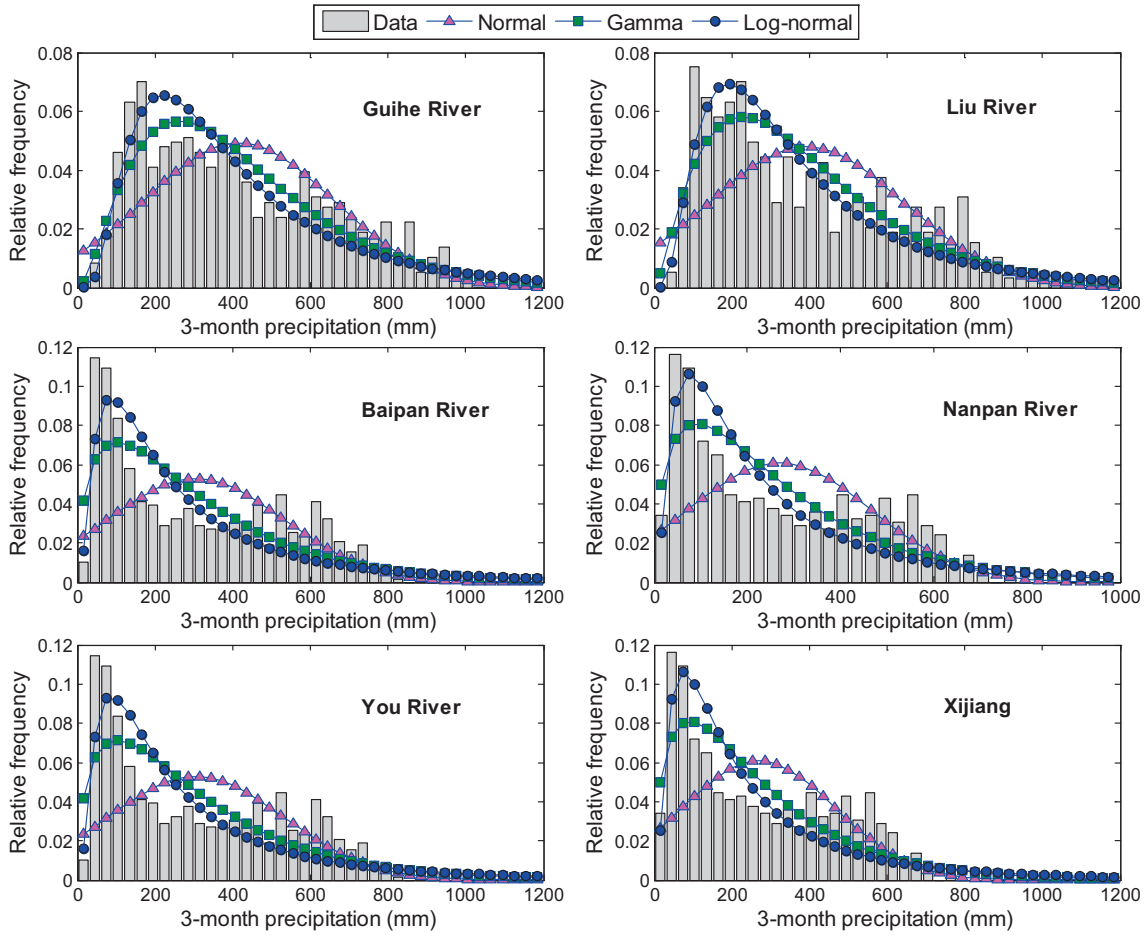

Fig. 3. Comparison of three probability distributions with the histogram of 3-month precipitation data for 5 headwater sub-basins and the whole Xijiang basin.

1° × 1° spatial resolution. The daily forcing data for the period of 2001–2010 were derived from 32 national standard rainfall stations within the Xijiang basin and gridded to 0.5° × 0.5° grid cells. The soil and vegetation data sets provided in Nijssen et al. (2001) were directly used, and no further calibration is performed for the VIC model simulations. For the two periods (1951–2000 and 2001–2010), two years, 1951 and 2001, serve as the model spin-up time, and the daily time series of major hydrological components (i.e., evapotranspiration, runoff, and soil moisture) were obtained as model outputs respectively. In the present study, monthly time series of runoff and soil moisture are derived from the simulated terrestrial hydrological data for both whole-basin/sub-basin area and grid cells.

The runoff simulations over the Xijiang basin were validated by two streamflow gauging stations (i.e., Gaoyao and Wuzhou) in Niu and Chen (2010), and another four (i.e., Liuzhou, Zhedong, Baise, and Nanning) in Niu et al. (2014). The comparison results between the observations and simulations for those six stations, by employing three objective functions, relative bias (RB), relative root mean square error (RRMSE), and Nash-Sutcliffe efficiency (NSE), are listed in Appendix A. The values of statistical items show that the VIC model can simulate reasonably the runoff for the control stations of the Xijiang basin and its several sub-basins. The model performance at monthly time scale is evaluated as "satisfactory" (NSE > 0.5 and RB < ± 0.25), according to the performance ratings suggested by Moriasi et al. (2007).

The simulated soil moisture by the VIC model is compared with the re-analysis outputs provided by the National Center for Environmental Prediction – National Center for Atmospheric Research (NCEP-NCAR) re-analysis-1(R-1) and the National Center for Environmental Prediction – Department of Energy (NCEP-DOE) re-analysis-2(R-2). R-1 has soil moisture data started in 1950 at a horizontal resolution about 210 km. R-2 is an updated version of R-1 with reducing human errors and improving soil wetness (Kanamitsu et al., 2002; Li et al., 2005), but only available from 1979. Since the range of total soil depths in the VIC model for the Xijiang basin is 1.5–3 m, the top 1.5 m is adopted for the comparison with the re-analysis data. The R-1/R-2 anomaly soil moisture data are obtained by five steps: (1) spatially aggregating from gridded (about 1.875° × 1.875°) to the whole Xijiang basin area; (2) the removing of the value corresponding to 29 February in leap years; (3) the removing of the corresponding annual cycle (i.e., 365 daily mean); (4) the scaling of the total 2 m to the upper 1.5 m; (5) the converting of the volumetric soil moisture to soil water. Fig. 2 shows the comparisons of the soil moisture anomaly for the Xijiang basin between the VIC model simulations and the R-1 and R-2 outputs for the period of 2002–2010. It is observed that the variation of the model simulations is between that of R-1 and R-2 data. Meanwhile, Fig. 2 displays the difference between the time series of R-1 and R-2 for the studied region, which indicates the difficulty and uncertainty of simulating soil moisture.

The limitation of utilizing simulated soil moisture data is that the model uncertainty certainly will impact the computation of relevant drought indices. Large differences in soil moisture and evapotranspiration from varying land surface models have been found (Long et al., 2013; Long et al., 2014). The use of VIC model in the present study for the Xijiang River basin is considered particularly because of its ability to simulate, with grid-based data,

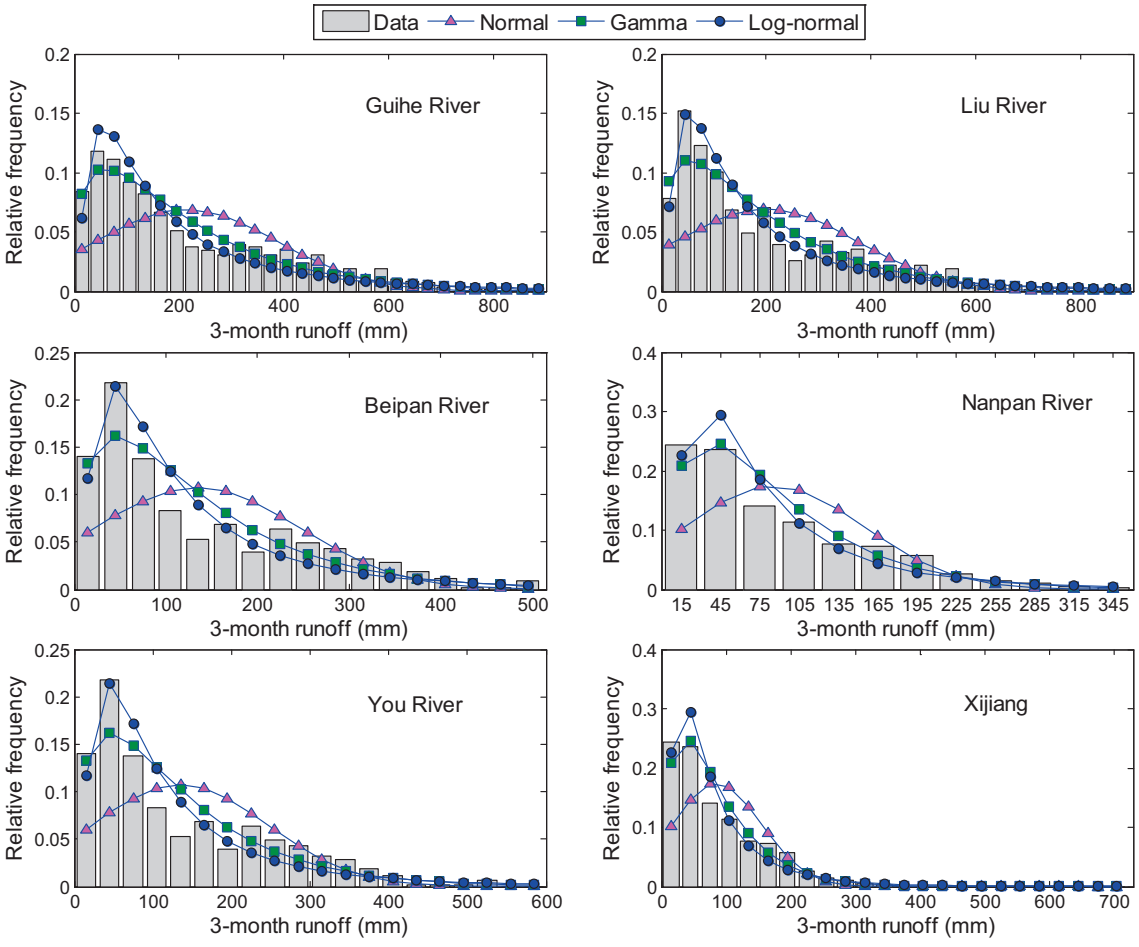

Fig. 4. Same as Fig. 3 but for runoff.

hydrological processes over the very large area of the whole Xijiang basin, with reasonable validations of runoff observations from gauge stations and the water balance of major hydrological components (Niu and Chen, 2010; Niu et al., 2014).

3. Methods

With due consideration of the selection priority (Keyantash and Dracup, 2002) of the drought indices (e.g., robustness, tractability, and dimensionality) for a large-scale river basin, the standardized precipitation index (SPI) (McKee et al., 1993) and the standardized runoff index (SRI) (Shukla and Wood, 2008) were employed to examine the meteorological drought and hydrological drought respectively in the present study. The VIC model output, soil moisture, is generally less validated compared to the runoff. The soil moisture anomaly index (SMAI) (Bergman et al., 1988) is selected here for inspecting agricultural drought, as it is a simple transformation of soil moisture data. Further, the SMAI is also proper for the comparisons over different grid cells.

3.1. Standardized precipitation/runoff index (SPI/SRI)

The procedures of computing the SPI and SRI are the same in the present study, which includes the following steps. (1) A probability distribution is fit to the sample; (2) the distribution is used to estimate the cumulative probability of the precipitation/runoff value; and, (3) the cumulative probability is converted to a standard normal deviation, with a mean of zero and standard deviation of unity. Different spatial aggregations (e.g., sub-basin) and different durations (e.g., 3-month) can be pursued based on source data resolution for the desired application (Shukla and Wood, 2008). Following the definition in McKee et al. (1993), a drought event occurred during a period in which the index value is continuously negative and reaches a value of −0.10 or less. The drought severity is arbitrarily defined for index values with different categories, such as the extreme drought for the value less than −2.0.

The similar notes to the SPI calculation are considered for the SRI computation. Ideally a continuous period of at least 30 years data set is preferred (McKee et al, 1993) to select the probability distribution. Angelidis et al. (2012) recommended the consistent data length for the SPI comparison at different studied regions. Regarding the issue of zero value in the sample, there is no zero value for the monthly precipitation/runoff value in the Xijiang basin for the studied periods. Zhang et al. (2009) reported that Log-normal is suitable to describe the distribution of monthly precipitation time series in the Pearl River basin South China. Shukla and Wood (2008) demonstrated that Log-normal distribution provides a better fit at high runoff values than Gamma distribution. Based on the previous studies, the present study examined the fitness of three probability density distributions, namely Normal, Log-normal, and Gamma, for the precipitation/runoff data in the Xijiang basin, and the Log-normal distribution is selected and performed in above step 1 (see Section 4.1 for the details) for a general consensus.

3.2. Soil moisture anomaly index (SMAI)

Different from the other indices for agricultural drought (e.g., CMI, Z), the SMAI approach is developed to characterize agricultural drought over a large area (Wu et al., 2011). The drought severity defined by SMAI is the relative departure of soil moisture from a normal climate condition, and the drought phenomenon is identified when the soil moisture deficit appears (i.e., the current soil moisture is less than the climatology soil moisture). Among them, the climatology soil moisture for a grid point or region is the average value for a multi-year dataset for the same time series. The relative soil moisture deficit is preferred because the dimensionality of the SMAI makes it suitable to compare drought severities in different periods at different grid points and regions, therefore over a large basin area.

4. Results and discussion

4.1. Probability density distribution

The comparisons of the three probability distributions with the histogram of the cumulative 3-month precipitation data, for the whole Xijiang basin and its 5 headwater sub-basins (i.e., the Guihe River, the Liu River, the Baipan River, the Nanpan River, and the You River basins), are given indicatively in Fig. 3. In each sub-figure, it covers 49-yr period (1952–2000) and contains 586 accumulation 3-month values. Overall, a satisfactory distribution is achieved by the Log-normal distribution, particularly to the precipitation in the Guihe River, the Liu River, and the whole basins. Fig. 4 also shows the Log-normal distribution fits better for the runoff data in the Xijiang basin and its sub-basins.

The probability distributions for the observed precipitation and simulated runoff at 4 timescales (1-, 2-, 3-, and 12-month) are further compared. The Kolmogorov–Smirnov (K–S) test (see Appendix B for the method description) is performed to examine the goodness-of-fit of the Normal, Gamma, and Log-normal distributions. The K-S test is employed as it is a robust and simple formalism (Georgakakos et al., 2005; Angelidis et al., 2012). The testing results for precipitation/runoff data, over 5 headwater sub-basins and the whole basin, at the four timescales are listed in Table 1.

Table 1
Fitting three theoretical probability distributions (Normal, Gamma, and Log-normal) for observed precipitation and simulated runoff at 1-, 3-, 6-, and 12-month timescales, with Kolmogorov–Smirnov (K–S) test.

Sub-basins	1-month			3-month			6-month			12-month		
	Normal	Gamma	Log-normal	Normal	Gamma	Log-normal	Normal	Gamma	Log-normal	Normal	Gamma	Log-normal
	Precipitation*											
Guihe River		√			√	√	√		√	√	√	√
Liu River		√	√		√	√			√	√	√	√
Baipan River										√	√	√
Nanpan River										√	√	√
You River										√	√	√
Xijiang										√	√	√
	Runoff*											
Guihe River			√		√	√		√	√	√	√	√
Liu River			√			√			√	√	√	√
Baipan River									√	√	√	√
Nanpan River			√			√		√	√	√	√	√
You River			√			√		√	√	√	√	√
Xijiang		√	√			√				√	√	√

* √: Distribution acceptable to fit data at confidence level 99%; shaded cell: the optimum distribution fitting to data.

The symbol √ indicates that the precipitation or runoff time series for a specific timescale passes the K-S test for a chosen level of confidence (1-a) = 0.99; the shaded area stands for the optimum distribution that fits better among the three distributions, on the basis of the largest vertical distance *Diff* between the empirical and three theoretical probability distributions. Table 1 indicates that the Log-normal and Gamma seem to fit better at 1- and 3-month timescales for observed precipitation, and Normal distribution begins to be acceptable at relatively higher timescales (6- and 12-month). The suitability of Log-normal distribution is basically more reflected for simulated runoff over all timescales. As the timescale increases, the representations of the three distributions tend to be equally well, which is consistent with the conclusions on 76-year (1931–2007) precipitation data from National Information System for the Water Resources of Portugal (Angelidis et al., 2012) and from a drought climatology analysis for the period of 1901–1999 over the European region by Lloyd-Hughes and Saunders (2002).

4.2. Spatio-temporal features

The monthly time series of the SPI and SRI for four accumulation periods (1-, 3-, 6- and 12-month) during 1952–1985 are shown in Fig. 5 collectively, which illustrate the differences in the behavior of the two indices derived from areal averages of observed precipitation and the VIC simulated runoff in the Nanpan River basin (i.e., the westernmost sub-basin). It is observed that, at 1-month timescale, the variation of SRI is less than that of SPI, especially during the drought episodes (i.e., where the index value less than 0). This is mainly due to the buffer behavior of land surface to the precipitation variability, resulting in that the drought severity in hydrological drought reflected by the runoff index is lower than that of meteorological drought represented by the precipitation index. The differences between SPI and SRI decrease as the accumulation period increases. The 12-month SPI and SRI are very consistent as shown in Fig. 5. These are generally consistent with the study of Shukla and Wood (2008) on the Feather River basin in California. Moreover, the SPI or SRI at longer timescale includes more antecedent effects of precipitation or runoff. For example, the drought severity in 1963 for 6-month period index is higher than those of 1- and 3-month. For the 12-month period, the high drought severity appears in 1963–1964, because it also incorporates the drought process in the wet season in 1963. Table 2 lists the correlations between SPI and SRI in 5 headwater sub-basins for the total period of 1952–2010 (left value). The correlation values increase along the timescales for the basins, as demonstrated by the average correlation between SPI and SRI changed from 0.837 (at 1-month timescale) to 0.936 (at 12-month timescale).

Table 2 also presents the correlations between SPI and SRI for the wet season (i.e., April–September) (middle value) and winter (i.e., December, January, February) (right value) (representing the dry season) for the sub-basins. For a specific timescale 3-month, the Liu River basin has the largest correlation value (0.949) in wet season, and the You river basin shows the lowest correlation value (0.765) in winter. The Liu River basin (i.e., the north central sub-basin in the Xijiang basin) is characterized as a fan-like basin shape and convergence river network (see Fig. 1). Compared to other sub-basins, more high-frequency precipitation is conserved by runoff, partly due to the geographical features. Fig. 6 shows

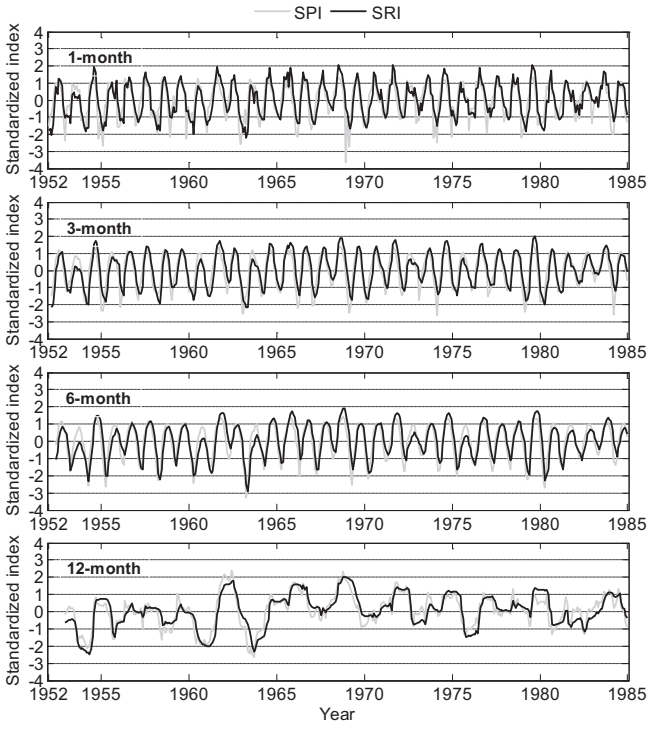

Fig. 5. The derived 1-, 3-, 6-, and 12-month SPI and SRI from observed precipitation and VIC simulated runoff in the Nanpan River basin.

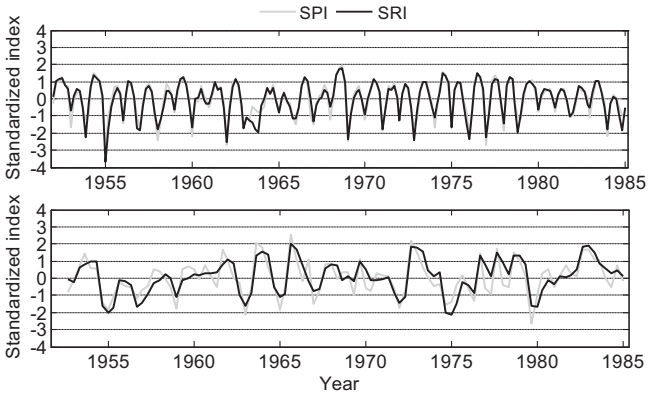

Fig. 6. The 3-month SPI and SRI for the wet season (April–September, upper panel) and winter (December, January, and February; lower panel) in the Liu River basin.

Table 2
Correlations between the SRI and SPI (for total period/wet season/winter) at different timescales over different headwater sub-basins.

Sub-basins	1-month Total/wet/winter	3-month Total/wet/winter	6-month Total/wet/winter	12-month Total/wet/winter
Guihe River	0.85/0.89/0.64	0.92/0.92/0.84	0.95/0.95/0.88	0.96/0.97/0.95
Liu River	0.87/0.90/0.58	0.94/0.95/0.82	0.96/0.96/0.91	0.96/0.97/0.96
Baipan River	0.83/0.86/0.31	0.88/0.95/0.83	0.89/0.93/0.88	0.94/0.92/0.97
Nanpan River	0.81/0.87/0.42	0.85/0.94/0.80	0.86/0.90/0.81	0.90/0.86/0.94
You River	0.83/0.81/0.42	0.88/0.94/0.77	0.88/0.93/0.85	0.91/0.90/0.93

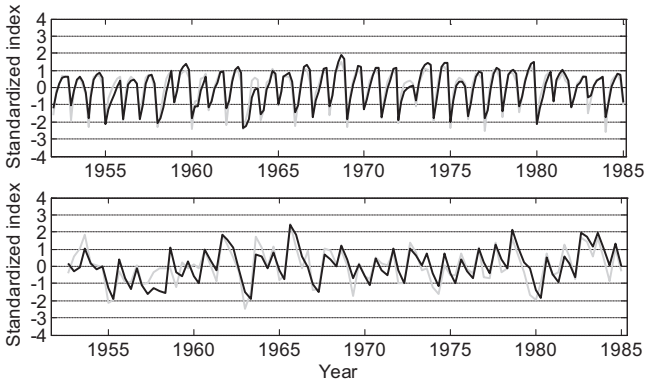

Fig. 7. Same as Fig. 6 but for the You River basin.

3-month period SPI and SRI for both the wet season and winter for the Liu river basin. In the wet season, the SRI displays more consistency with SPI in the upper panel of Fig. 6. The mainstream of the You River basin is longer due to the long-narrow basin shape and the basin's river network is distributed, which contribute the delay response of runoff and soil moisture to precipitation variability (Niu and Chen, 2014). Therefore, the time lag can be noticed between SPI and SRI, such as the drought years 1957, 1963, 1973, and 1979, shown in the lower panel of Fig. 7.

In exploring the impacts of "basin-scale topography" on drought pattern changes, we strengthened here it on the aspects of basin shape and river network distribution, as the 1 or 0.5 degree spatial resolution is still a "large-scale" for studying the impacts of local slope. Nevertheless, the spatio-temporal evolutions, on the large-scale grid-cell basis we studied, can be attributed to the overall slope of sub-basin, which we think would have been partly represented in the factor of basin shape.

4.3. Drought evolution

The most severe drought event in the period of 2002–2010 for the Xijiang basin occurred on in March 2010 (Niu et al., 2013). Fig. 8 shows the 3-month period SPI and SRI, from February to April, based on 168 grid cells ($0.5° \times 0.5°$), to characterize the drought evolution processes from meteorological drought to hydrological drought. In February, the center of drought zone indentified by SPI mainly locates at the juncture between Yunnan province (its capital Kunming City) and Guizhou province (its capital Guiyang City) with higher elevation. The center of the hydrological drought is located at the south of Guizhou province and the east part of Yunnan province (i.e., the upstream of the Hongshui River and the Nanpan River). Meanwhile, the drought severity described by SRI is less than that of SPI. Generally, the evapotranspiration is relatively lower at high elevation area due mostly to relatively lower soil moisture availability and lower temperature,

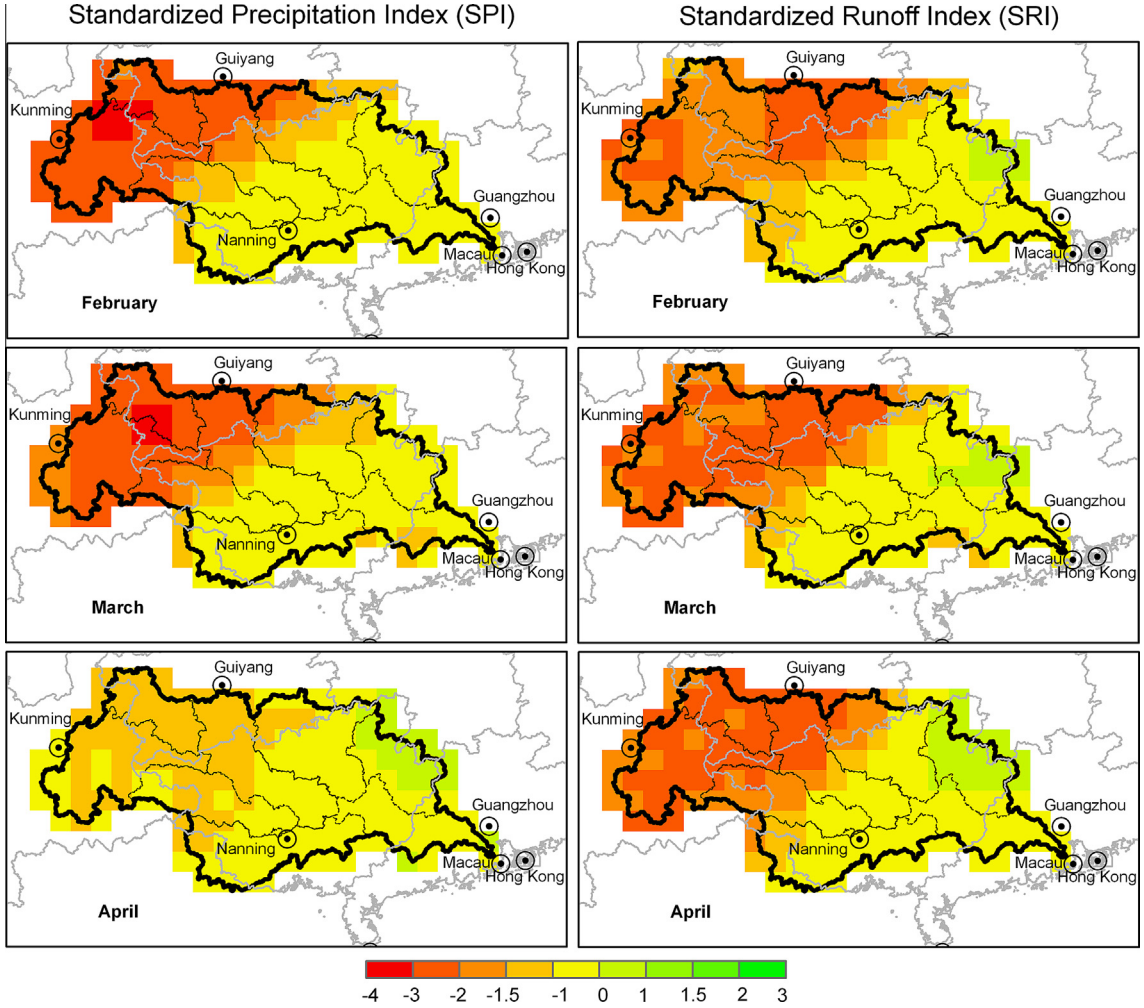

Fig. 8. The 3-month SPI and SRI from February to April in 2010 over the Xijiang basin as derived from observed precipitation and VIC simulated runoff.

which results in the runoff deficit not that significant compared with that of precipitation. Therefore, the SRI is relatively lower than SPI for the region. It is noted that net radiation and land cover could also induce variations in partitioning of precipitation into runoff and evapotranspiration (Long et al., 2010; Long et al., 2014). The center of the meteorological drought gradually moved the east in March, and the severest drought area reflected by SRI is expanded to the lower reach of the Nanpan River basin. In April, the meteorological drought was recovered to a certain degree compared to that in March, but the reduction of drought severity is not obvious for the hydrological drought, especially for the west part of the Xijiang basin. These also indicate the spatial evolution differences between SPI and SRI for the basin.

Although the simulated soil moisture is farther to being a verified product from the VIC model than runoff in the present study, we examine the agricultural drought through soil moisture fluxes as a useful complement. Fig. 9 shows the SMAI in the unit of percentage (%), derived from the simulated top 1-m soil moisture data at $0.5^\circ \times 0.5^\circ$ spatial resolution and further interpolated over the Xijiang basin, from February 2010 to April 2010. The center of agricultural drought roughly locates the juncture of the Hongshui River, the Baipan River, the Nanpan River and the You River basins for the three months. The severest agricultural drought occurred in March, which is consistent with hydrological drought. More spatial consistency in terms of the severe drought area between SRI and SMAI appears on the severest drought period, i.e., March. Similar to the hydrological drought, the agricultural drought has lower recession speed compared to meteorological drought from March to April.

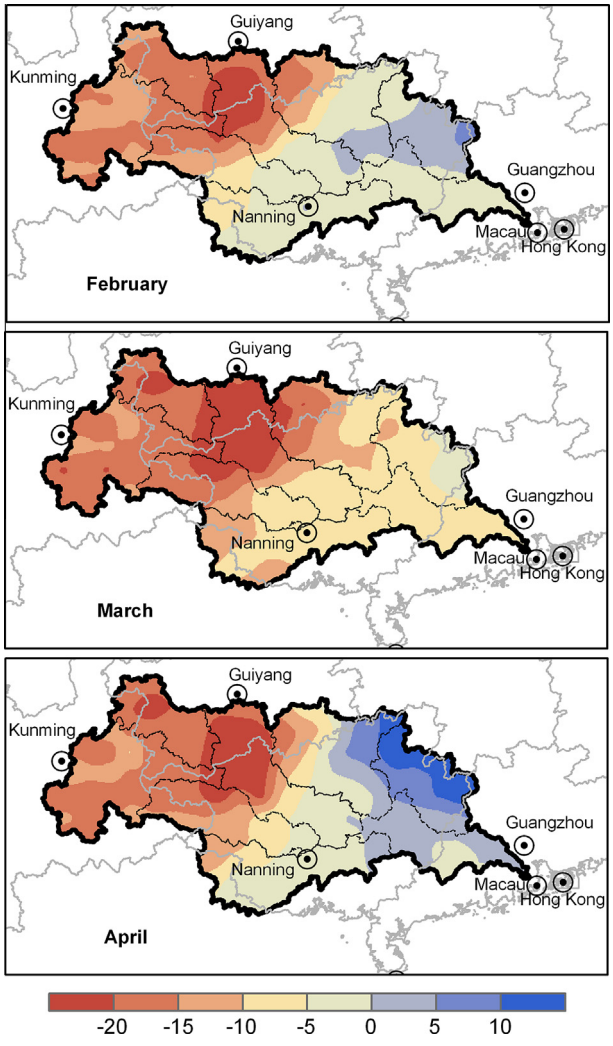

Fig. 9. The SMAI derived from the simulated top-1 m soil moisture from February to April in 2010 over the Xijiang basin.

It is also noted that the SRI and SMAI calculations here are from the macro-scale hydrological modeling. It is difficult to consider the operation effects of local lakes and reservoirs due to its inherently large-scale features. In these cases, for small interested region where exits heavy reservoir operation in the upstream reach, more local anthropogenic effect data should be incorporated and studied for detailing the drought evolution at small spatial scale.

5. Conclusions

The drought processes in the Xijiang basin were investigated by the drought indices on the sub-basin and grid cell basis. The spatio-temporal differences between SPI and SRI were revealed, which display the drought evolution characteristics from meteorological drought to hydrological drought. The drought severity, described by SRI and SPI at 1-, 3-, 6- and 12 month, shows more consistency with timescale increase in the Xijiang basin and its headwater sub-basins; since the high-frequency precipitation variability is less attenuated by runoff in the Liu River basin, the hydrological drought evolution reflected by SRI is close to that of SPI in wet season for the sub-basin; the time lag between SRI and SPI appears in the You river basin, partly due to the long narrow basin shape of the sub-basin.

The differences of drought severity over the grid cells in the Xijiang basin are also disclosed, by employing SPI, SRI and SMAI, in depicting the 2010 spring drought event. The basin-scale topography is an important factor to regulate the spatial and temporal processes of drought evolution in the studied region: the basin with fan-like basin shape and converged river network (e.g., the Liu River and the Guihe River basins) may have active response to precipitation variability. Therefore, more consistency between meteorological drought and hydrological drought occurs; the hydrological drought severity is less than meteorological drought severity for the area with high elevation during the drought developing stage; the spatial consistency on severe drought area between hydrological drought and agricultural drought appears more during the severest drought period; the recession of hydrological and agricultural drought severity is behind that of meteorological drought for the longer mainstream basin (e.g., the You River and the Nanpan River basins).

Macro-scale hydrological modeling has been effectively advanced in the last two decades, and runoff is a relatively easy-validated variable compared to the other model output (e.g., soil moisture). The SPI has been widely used due to its simplicity on both source data obtainment and computation procedures, and the calculation of SRI is similar to SPI based on the simulated runoff data. Therefore, SRI would be easily applied in the drought-related research, monitoring, and management, and further improve our understanding of the drought processes for a large-scale river basin. Although the simulated soil moisture is generally less validated due to the availability of observed soil moisture data, it is a useful complement to describe the drought evolution, as illustrated with the utilization of SMAI in the present study.

Acknowledgments

The authors are grateful to the financial support provided by the National Natural Science Foundation of China (Grant No.: 51309198) and two General Research Fund (GRF) Projects (No.: HKU 710712E and 7109010E) from the Research Grants Council of Hong Kong. Many thanks to two anonymous reviewers and

Table A.1
Model validation results at a monthly timestep for 6 gauging stations over the Xijiang basin (in Fig. 1) (adapted from Niu and Chen (2014)).

River	Station	Control area (km^2)	Period	RB	RRMSE	NSE
Xijiang Lower Reach	Gaoyao	351,525	1980–2000	0.06	0.27	0.88
Xijiang Lower Reach	Wuzhou	329,705	1981–1985	0.01	0.20	0.90
Baipan River	Zhedong	19,300	1958–1987	−0.02	0.59	0.72
You River	Baise	21,930	1951–1985	0.12	0.52	0.78
Zuoyu River	Nanning	75,520	1951–1985	0.26	0.45	0.80
Liu River	Liuzhou	45,785	1951–1987	−0.09	0.32	0.90

associate editor, for the valuable comments and suggestions, which helped improve an earlier version of this manuscript.

Appendix A

See Table A.1.

Appendix B

The Kolmogorov–Smirnov goodness-of-fit (Chakravarti et al., 1967; Melesse et al., 2010) is used to test the probability distribution for observed precipitation and simulated runoff data. For a random group of samples (x_1, x_2, …, x_n), the empirical cumulative distribution function (F_e) is defined as:

$$F_e(x_i) = \frac{n_l}{n} \tag{B.1}$$

where n_l is the number of data less than x_i, and the series of x_i are ordered from the smallest to the largest. The Kolmogorov-Smirnov test is based on evaluation of F_e. The test statistic (Melesse et al., 2010) is the largest vertical difference (*Diff*) between F_e and the theoretical cumulative distribution function (F_t):

$$Diff = \max_{1\leqslant i\leqslant n}\left(F_t(x_i) - F_e(x_i), F_e(x_i) - F_t(x_i) + \frac{1}{n}\right) \tag{B.2}$$

By comparing with the expected maximum difference at a specified confidence level (e.g., 99% used in this study), the null hypothesis of no difference is tested.

References

Andreadis, K.M., Lettenmaier, D.P., 2006. Trends in 20th centry drought over the continental United States. Geophys. Res. Lett. 33, L10403. http://dx.doi.org/10.1029/2006GL025711.

Angelidis, P., Maris, F., Kotsovinos, N., Hrissanthou, V., 2012. Computation of drought index SPI with alternative distribution functions. Water Resour. Manage. 26, 2453–2473.

Bergman, K.H., Sabol, P., Miskus, D., 1988. Experimental indices for monitoring global drought conditions. In: Proc. 13th Annual Climate Diagnostics Workshop, Cambridge, MA, US Dept. of Commerce, pp. 190–197.

Bhalme, H.N., Mooley, D.A., 1980. Large-scale droughts/floods and monsoon circulation. Monthly Weather Rev. 108, 1197–1211.

Chakravarti, L., Laha, R.G., Roy, J., 1967. Handbook of Methods of Applied Statistics. John Wiley and Sons, New York.

Chen, J., Kumar, P., 2001. Topographic influence on the seasonal and interannual variation of water and energy balance of basins in North America. J. Clim. 14 (9), 1989–2014.

Chen, J., Wu, Y., 2012. Advancing representation of hydrologic processes in the Soil and Water Assessment Tool (SWAT) through integration of the TOPographic Model (TOPMODEL) features. J. Hydrol. 420, 319–328.

Chen, J., Niu, J., Sun, L., 2013. Water resources of mainland China. In: Pielke Sr, Roger (Ed.), Climate Vulnerability: Understanding and Addressing Threats to Essential Resources, vol. 5. Elsevier, pp. 195–211. http://dx.doi.org/10.1016/B978-0-12-384703-4.00527-X.

Cui, W.Z., Chen, J., Wu, Y.P., Wu, Y.D., 2007. An overview of water resources management of the Pearl River. Water Sci. Technol.: Water Supply 7 (2), 101–113.

Dai, A., 2011. Drought under global warming: a review. WIREs Clim. Change 2, 45–65.

Federal Emergency Management Agency, 1995. National Mitigation Strategy: Partnerships for Building Safer Communities. Federal Emergency Management Agency, Washington, DC, pp. 26.

Feng, S., Hu, Q., Qian, W.H., 2004. Quality control of daily meteorological data in China, 1951–2000: a new dataset. Int. J. Climatol. 24, 853–870.

Fischer, T., Gemmer, M., Su, B., Scholten, T., 2013. Hydrological long-term dry and wet periods in the Xijiang River basin, South China. Hydrol. Earth Syst. Sci. 17, 135–148.

Georgakakos, K., Bae, D.-H., Jeong, C.-S., 2005. Utility of ten-day climate model ensemble simulations for water resources applications in Korean watersheds. Water Resour. Manage. 19, 849–872.

Heim Jr., R.R., 2002. A review of twentieth-century drought indices used in the United States. Bull. Am. Meteorol. Soc. 83 (8), 1149–1165.

Huang, J., Van den Dool, H.M., Georgakakos, K.P., 1996. Analysis of model-calculated soil moisture over the United States (1931–1999) and applications to long-range temperature forecasts. J. Clim. 9, 1350–1362.

Kanamitsu, M., Ebisuzaki, W., Woollen, J., Yang, S.-K., Hnilo, J.J., Florino, M., Potter, G.L., 2002. NCEP–DOE AMIP–II reanalysis (R-2). Bull. Am. Meteorol. Soc. 83, 1631–1643.

Keyantash, J., Dracup, J.A., 2002. The quantification of drought: an evaluation of drought indices. Bull. Am. Meteorol. Soc. 83, 1167–1180.

Kunkel, K.E., 1990. Operational soil moisture estimation for the midwestern United States. J. Appl. Meteorol. 29, 1158–1166.

Li, H.B., Robock, A., Liu, S.X., Mo, X.G., Viterbo, P., 2005. Evaluation of reanalysis soil moisture simulations using updated Chinese soil moisture observations. J. Hydrometeorol. 6, 180–193.

Liang, X., Lettenmaier, D.P., Wood, E.F., Burges, S.J., 1994. A simple hydrologically based model of land surface water and energy fluxes for general circulation models. J. Geophys. Res. 99, 14415–14428.

Lloyd-Hughes, B., Saunders, M.A., 2002. A drought climatology for Europe. Int. J. Climatol. 22, 1571–1592.

Long, D., Gao, Y.C., Singh, V.P., 2010. Estimation of daily average net radiation from MODIS data and DEM over the Baiyangdian watershed in North China for clear sky days. J. Hydrol. 388 (3–4), 217–233.

Long, D., Scanlon, B.R., Longuevergne, L., Sun, A.-Y., Fernando, D.N., Save, H., 2013. GRACE satellite monitoring of large depletion in water storage in response to the 2011 drought in Texas. Geophys. Res. Lett. 40 (13), 3395–3401.

Long, D., Longuevergne, L., Scanlon, B.R., 2014. Uncertainty in evapotranspiration from land surface modeling, remote sensing, and GRACE satellites. Water Resour. Res. 50 (2), 1131–1151.

Maurer, E.P., Wood, A.W., Adam, J.C., Lettenmaier, D.P., Nijssen, B., 2002. A long-term hydrologically based dataset of land surface fluxes and states for the conterminous United States. J. Clim. 15, 3237–3251.

McKee, T.B., Doesken, N.J., Kleist, J., 1993, The relationship of drought frequency and duration to timescales. In: Paper presented at 8th Conference on Applied Climatology, 17–22 Jan, 1993, Anaheim, California.

Melesse, A., Abtew, W., Dessalegne, T., Wang, X.X., 2010. Low and high flow analysis and wavelet application for characterization of the Blue Nile River system. Hydrol. Process. 24, 241–252.

Mishra, A.K., Singh, V.P., 2009. Analysis of drought severity-area-frequency curves using a general circulation model and scenario uncertainty. J. Geophys. Res. 114, D06120. http://dx.doi.org/10.1029/2008JD010986.

Mishra, A.K., Singh, V.P., 2010. A review of drought concepts. J. Hydrol. 391 (1–2), 201–216.

Mishra, A.K., Desai, V.R., Singh, V.P., 2007. Drought forecasting using a hybrid stochastic and neural network model. J. Hydrol. Eng. 12 (6), 626–638.

Moriasi, D.N., Arnold, J.G., Van Liew, M.W., Bingner, R.L., Harmel, R.D., Veith, T.L., 2007. Model evaluation guidelines for systematic quantification of accuracy in watershed simulations. Trans. ASABE 50 (3), 885–990.

Nijssen, B., Lettenmaier, D.P., Liang, X., Wetzel, S.W., Wood, E.F., 1997. Streamflow simulation for continental-scale river basins. Water Resour. Res. 33 (4), 711–724.

Nijssen, B., Schnur, R., Lettenmaier, D.P., 2001. Global retrospective estimation of soil moisture using the VIC land surface model. J. Clim. 14, 1790–1808.

Niu, J., 2013. Precipitation in the Pearl River basin, South China: scaling, regional patterns, and influence of large-scale climate anomalies. Stochastic Environ. Res. Risk Assess. 27 (5), 1253–1268. http://dx.doi.org/10.1007/s00477-012-0661-2.

Niu, J., Chen, J., 2010. Terrestrial hydrological features of the Pearl River basin in South China. J. Hydro-environ. Res. 4, 279–288. http://dx.doi.org/10.1016/j.jher.2010.04.016.

Niu, J., Chen, J., 2014. Terrestrial hydrological responses to precipitation variability in Southwest China with emphasis on drought. Hydrol. Sci. J. 59 (2), 325–335. http://dx.doi.org/10.1080/02626667.2013.822641.

Niu, J., Chen, J., Sun, L., 2013. Major drought events in the West River basin in South China for the period of 2002–2010. In: Wang, Z.Y., Lee, J.H.W., Gao, J.Z., Cao, S.Y. (Eds.). Proceeding of the 35th IAHR World Congress. 8–13 September, 2013, Chengdu, China.

Niu, J., Chen, J., Sivakumar, B., 2014. Teleconnection analysis of runoff and soil moisture over the Pearl River basin in southern China. Hydrol. Earth Syst. Sci. 18, 1475–1492. http://dx.doi.org/10.5194/hess-18-1475-2014.

Özger, M., Mishra, A.K., Singh, V.P., 2009. Low frequency drought variability with climatic indices. J. Hydrol. 364, 152–162.

Palmer, W.C., 1965. Meteorological drought. Research Paper No.45, U.S. Department of Commerce, Washington, D.C., pp. 58.

Palmer, W.C., 1968. Keeping track of crop moisture conditions, nationwide: the new crop moisture index. Weatherwise 21, 156–161.

Pearl River Hydraulic Research Institute, 2007. Drought Monitor and Assessment Reports for the Pearl River Basin using Remote Sensing. Pearl River Hydraulic Research Institute, Guangzhou, pp. 60 (in Chinese).

Pearl River Water Resources Commission, 2005. Pearl River Flood Prevention Handbook. Pearl River Water Resources Commission, Guangzhou, pp. 150 (in Chinese).

Shafer, B.A., Dezman, L.E., 1982. Development of a Surface Water Supply Index (SWSI) to assess the severity of drought conditions in snowpack runoff areas. In: Proc. 50th Western Snow Conf., Reno, NV, pp. 164–175.

Sheffield, J., Eric, F.W., 2008. Global trends and variability in soil moisture and drought characteristics, 1950–2000, from observation-driven simulations of the terrestrial hydrologic cycle. J. Clim. 21, 432–458.

Sheffield, J., Goteti, G., Wen, F.H., Wood, E.F., 2004. A simulated soil moisture based drought analysis for the United States. J. Geophys. Res. 109, D24108. http://dx.doi.org/10.1029/2004JD005182.

Shukla, S., Wood, A.W., 2008. Use of a standardized runoff index for characterizing hydrologic drought. Geophys. Res. Lett. 35, L02405. http://dx.doi.org/10.1029/2007GL032487.

Soulé, P.T., 1992. Spatial patterns of drought frequency and duration in the contiguous USA based on multiple drought event definitions. Int. J. Climatol. 12, 11–24.

Svoboda, M., LeComte, D., Hayers, M., Heim, R., Gleason, K., Angel, J., Rippey, B., Tinker, R., Palecki, M., Stooksbury, D., Miskus, D., Stephens, S., 2002. The drought monitor. Bull. Am. Meteorol. Soc. 83, 1181–1190.

van Rooy, M.P., 1965. A rainfall anomaly index independent of time and space. Notos 14, 43–48.

Wilhite, D.A., 2000. Drought as a natural hazard: Concepts and definitions. Drought: A Global Assessment. In: Wilhite, D.A., (Ed.), Routledge, pp. 3–18.

Wu, Z.Y., Lu, G.H., Wen, L., Lin, C.A., 2011. Reconstructing and analyzing China's fifty-nine year (1951–2009) drought history using hydrological model simulation. Hydrol. Earth Syst. Sci. 15 (1), 2881–2894.

Xiao, M.Z., Zhang, Q., Chen, X.H., 2012. Regionalization and changing properties of drought events along the Pearl River basin. J. Catastrophol. 27 (3), 12–18 (in Chinese).

Zhang, S.R., Lu, X.X., Higgitt, D.L., Chen, C.A., Han, J.T., Sun, H.G., 2008. Recent changes of water discharge and sediment load in the Zhujiang (Pearl River) basin, China. Glob. Planet. Change 60, 365–380.

Zhang, Q., Xu, C.Y., Zhang, Z.X., 2009. Observed change of drought/wetness episodes in the Pearl River River basin, China, using the standardized precipitation index and aridity index. Theor. Appl. Climatol. 98, 89–99.

Zhang, Q., Xiao, M.Z., Singh, V.P., Chen, X.H., 2013. Copula-based risk evaluation of droughts across the Pearl River basin, China. Theor. Appl. Climatol. 111, 119–131.